Enhanced Vertical Ordering of Block Copolymer Films by Tuning Molecular Mass

ARTICLE *in* RSC ADVANCES · MARCH 2015

Impact Factor: 3.84 · DOI: 10.1039/C5RA02047F

4 AUTHORS, INCLUDING:

Xiaohua Zhang
Soochow University (PRC)
28 PUBLICATIONS **364** CITATIONS
SEE PROFILE

J. F. Douglas
National Institute of Standards and Techno…
428 PUBLICATIONS **14,795** CITATIONS
SEE PROFILE

Alamgir Karim
University of Akron
307 PUBLICATIONS **6,938** CITATIONS
SEE PROFILE

RSC Advances

PAPER

Cite this: *RSC Adv.*, 2015, **5**, 32307

Enhanced vertical ordering of block copolymer films by tuning molecular mass†

Xiaohua Zhang,*[a] Jack F. Douglas,*[b] Sushil Satija[c] and Alamgir Karim*[d]

We demonstrate that an increase in the molecular mass (chain length N) of a cylinder-forming PS–PMMA block copolymer (BCP), and thus the Flory–Huggins interaction strength χN, allows us to form well-organized surface patterns having the technologically interesting perpendicular cylinder BCP orientation with respect to the substrate. Tuning the polymer mass also allows for a precise control of the in-plane BCP cylinder pattern wavelength λ and gives rise to a local height variation of the BCP film in which the average film roughness varies in direct proportion to λ. At a fixed ordering temperature ($T = 182$ °C), we observe an orientation transition with increasing BCP molecular mass from a parallel to a perpendicular orientation. Based on the findings of the present work, and accumulated results from our former studies of BCP ordering, we propose as a *general principle* that increasing the BCP segregation strength by either lowering temperature or increasing the BCP mass, enhances the extent of vertical ordering in BCP thin films. We suggest that this effect arises because the segregation strength χN controls the shear rigidity of self-assembled BCP structures.

Received 2nd February 2015
Accepted 25th March 2015

DOI: 10.1039/c5ra02047f

www.rsc.org/advances

Introduction

Block copolymers (BCPs) self-assemble into a wide range of morphologies with periodicities in the order of 5 nm to 100 nm[1–4] and these interesting materials have been exhaustively studied because of the many potential applications envisioned from the use of these self-assembled nanoscale patterns. The control of nanodomain alignment in BCPs is essential for utilizing these materials as nanoscale templates for various nanotechnology fabrication applications[5,6] so that understanding the molecular and physical factors that can enhance the quality of ordering is a central scientific problem of importance for developing these materials for practical applications as lithographic templates and other applications.[7–11] Of course, when BCP films are confined to molecularly thin films, the ordering of BCP is significantly influenced by the interfacial energies of both the solid substrate and the air interface, making the control of the ordering morphology even more challenging because these boundary interactions must be quantified and controlled. Inevitably, the ordering of BCPs in thin films leads to a much 'richer' range of morphologies than bulk materials, a situation that offers opportunities along with the challenges of material characterization and the scientific understanding of principles required for morphology control.

A variety of strategies have been considered to enhance BCP ordering such as the use of external electric fields,[12–14] selective copolymer–substrate interactions,[15–18] shear fields,[19,20] solvent vapor treatment,[21,22] geometrical confinement,[23–26] zone refinement,[27–30] temperature gradients[31] and adjusting substrate surface roughness.[32–36] All of these methods have resulted in improved alignment of BCP domains, but the problem of developing an integrated effective strategy for engineering BCP alignment for thin BCP films remains a challenge.

Cylinder-forming BCPs are attracting increasing attention because of their potential importance in nanotechnology applications and the present work focuses on these materials. Cylinder-forming BCPs normally preferentially orient with the cylinders parallel to the substrate interface if there is any significant energetic preferences of either of the two blocks for the substrate or air interfaces. There has been much progress in understanding the formation of surface patterns in cylinder-forming block copolymers[37,38] that provide a starting point for the present work. Suh *et al.*[39] made an interesting scaling argument predicting a transformation from parallel cylinder orientation to a perpendicular configuration with respect to the supporting solid substrate in cylinder-forming block copolymer thin films when the thermodynamic driving force for BCP ordering is large. We observed such a transformation in a previous study of poly(styrene-*block*-methyl methacrylate) (PS-*b*-PMMA) copolymer forming cylinders thin films,[37] where we

[a]*Center for Soft Condensed Matter Physics and Interdisciplinary Research, Soochow University, Suzhou 215006, China. E-mail: zhangxiaohua@suda.edu.cn*

[b]*Materials Science and Engineering Division, Materials Measurement Laboratory, National Institute of Standards and Technology, Gaithersburg, Maryland 20899, USA. E-mail: jack.douglas@nist.gov*

[c]*NIST Center for Neutron Research, National Institute of Standards and Technology (NIST), Gaithersburg, Maryland 20899, USA*

[d]*Department of Polymer Engineering, University of Akron, Akron, Ohio 44325, USA*

further demonstrated that cylinder-forming BCPs exhibit a rich 'surface morphology diagram' which depends on ordering temperature, film casting method and film thickness. However, this earlier work did not explore other relevant processing variables such as substrate surface topography through the introduction of nanoparticles, an effect we have explored separately in the case of lamellae form BCP materials.[35] In our recent work on the alignment BCP lamellae in thin films, we also found that decreasing temperature greatly helped the achievement of a perpendicular lamellae orientation, provided the boundary interaction at the substrate is made nearly 'neutral' (*i.e.*, neither polymer block has a preferential affinity for the surface) and the temperature lowered to enhance the driving force for BCP ordering. This allowed for a tuning of the amount of BCP domains standing normal to the solid substrate by varying temperature. The present paper considers a similar strategy of enhancing the ordering in our cylinder-forming BCP films where we increase the thermodynamic driving force for ordering by increasing the BCP molecular mass. As in the low temperature lamellae-forming BCP films, we achieve a tunable orthogonal alignment of the BCP pattern on the substrate by enhancing the strength of the thermodynamic driving force for BCP ordering by simply varying the BCP molecular mass. This also allows for a precise tuning of the in-plane BCP pattern wavelength and local film height fluctuations in the ordered BCP film whose amplitude is linked to the in-plane pattern wavelength such that the ratio of these scales is an invariant. It seems likely that the control of these geometrical aspects of the BCP film structure should be important for applications in which topography as well as pattern wavelength are important, *e.g.*, response of cells to BCP coatings[40] for the preservation of blood, scattering of light, film frictional and adhesion properties, *etc.*

Experimental details

Preparation of BCP thin films

A series of PS-*b*-PMMA samples with different molar masses were obtained from various sources and used as received (Table 1).[41] PS-*b*-PMMA with $M_n = 40.5$ kg mol^{-1}, 47.7 kg mol^{-1} and 158 kg mol^{-1} have been purified and any traces amount of homopolymer are removed. The deuterated PS-*b*-PMMA (dPS-*b*-PMMA) BCPs with the total relative molecular mass of 77.5 kg mol^{-1} and 367.2 kg mol^{-1} were synthesized by Oak Ridge National Laboratory. dPS-*b*-PMMA is used to perform neutron reflectivity (NR) and small-angle neutron scattering (SANS) measurements. The scattering length densities (SLD) of protonated PMMA (hPMMA) and deuterated PS (dPS) blocks are 1.06×10^{-6} Å^{-2} and 6.38×10^{-6} Å^{-2}, respectively. The large contrast in SLD of hPMMA and dPS makes these ideal techniques for measuring the orientation of nanostructures of BCP over large areas. dPS-*b*-PMMA with $M_n = 77.5$ kg mol^{-1} and 367.2 kg mol^{-1} contain 1% and 2% (by mass) low molecular mass homopolymethylmethacrylate, respectively. For PS-*b*-PMMA the relatively high content of homopolymer (>15%) can influence the orientation of nanodomain.[42] In this study the effect of tiny amount of homopolymer (<2%) on the orientation of nanodomain is negligible. The influence of the compositional asymmetry on the nanodomain orientation in very thin (<55 nm) and highly asymmetric (20% mass fraction of PMMA) cylinder-forming PS-*b*-PMMA is significant.[43] In this work PS-*b*-PMMA has the mass fraction of PMMA in the range from 22% to 30% and the film thickness is above 96 nm. The compositional asymmetry of PS-*b*-PMMA did not show significant influence on the cylinder orientation. PS-*b*-PMMA films were prepared *via* flow coating[44] from the block copolymer solution in toluene onto the plasma-treated Si wafer. The procedure for generating a BCP film *via* flow coating is outlined as follows. A knife blade mounted on a metal holder was placed above the stage. The substrate is fixed to the translation stage beneath the blade. A fixed volume of polymer solution (50 μL for a 25 mm wide blade) is syringed along the leading edge of the knife blade, where polymer solution is held in place by capillary forces. The liquid film then dries to a solid film. The substrates used in this study are commercially-available atomically-flat Si wafers. The plasma-treated substrates are somewhat hydrophilic, which induces a preferential wetting behavior for the PMMA phase of the block copolymer. The film thickness, h_f, was characterized by ultraviolet-visible interferometry where the standard uncertainty of film thickness is ±1 nm. The BCP films were annealed in a vacuum oven.

Table 1 PS-*b*-PMMA molecular characterization information[a]

M_n (kg mol^{-1})	M_w/M_n	f_{PMMA}	Source
40.5	1.08	0.26	Polymer Source, Inc.
47.7	1.04	0.26	Polymer Source, Inc.
77.5	1.09	0.26	Oak Ridge National Laboratory
158.0	1.09	0.22	Polymer Source, Inc.
367.2	1.10	0.30	Oak Ridge National Laboratory

[a] f_{PMMA} is the mass fraction of PMMA.

Atomic force microscope (AFM)

AFM images were obtained in both height and phase modes with an Asylum MFP-3D scanning force microscope in its tapping mode. The tapping mode cantilevers with spring constant of ≈50 N m^{-1}, resonance frequency ranging from 100 kHz to 200 kHz, and the drive frequency with the offset of (−5%) were used. The phase image is the result of a convolution of variations in surface properties such as the local film elastic moduli along with tip adhesion and friction. In particular, the phase lag between the signal driving the cantilever to oscillate and the cantilever oscillation output signal is the source of the phase imaging. Despite the complex physical origin of this type of imaging, AFM imaging methods provides valuable insights into film structure, especially when combined with scattering or imaging measurements to further validate morphological assignments.

Height imaging is used to map the variations of the *z*-position of the tip during scanning, which are plotted as a

function of the x–y position of the tip to create our AFM height images. In the height imaging, the reduction of the oscillation amplitude is used to identify and estimate the dimensions of surface topographic features. The height imaging or 'topographic imaging' in combination with phase imaging is useful for discriminating local height variations from local variations in the mechanical properties of the polymer film. For PS-*b*-PMMA BCP thin films, the roughness of as-cast film and height variations in the ordered BCP films are obtained from height images of AFM. The influence of the mechanical properties of PS and PMMA phases on height image is not significant. To obtain the real space images of AFM, and to reduce imaging artifacts, the samples with the same annealing conditions were scanned in multiple positions in order to get more images at 2 μm × 2 μm.

Neutron reflectivity (NR)

The NR experiments were conducted at the NIST Center for Neutron Research at the National Institute of Standards and Technology. The NG7 horizontal reflectometer utilized a 4.76 Å collimated neutron beam with a wavelength divergence of 0.18 Å. The angular divergence of the beam was varied through the reflectivity scan and this provided a relative q resolution dq/q of 0.04, where $q = 4\pi \sin(\theta)/\lambda$, and θ is the incident and final angle with respect to the surface of the film. Scans were made over a wavevector magnitude (q) range from 0.075 $Å^{-1}$ to 0.12 $Å^{-1}$. Conversion of the NR spectra to the scattering length density (SLD) and concentration profiles was done using the NRSA software, a program provided by Charlie Laub (University of California, Davis).[45]

Small-angle neutron scattering (SANS). Rotational SANS experiments were conducted using the NG7-SANS instrument at the NIST Center for Neutron Research, using an incident wavelength of 6.0 Å and a wavelength divergence of 0.74 Å. The 2-D images are taken from a series of incidence angles and the measurements are made in transmission. Footprint corrections were applied by normalizing the scattering data using the intensity along the rotation axis (Q_y). Data was fit by extending the model of Ruland and Smarsly[46] to allow for both parallel and perpendicular populations of cylinders, each with an orientational distribution.

Results and discussion

In thin films, cylinder-forming PS-*b*-PMMA BCPs preferentially orient with the cylinders in a horizontal arrangement (parallel to the substrate interface) due to the energetic preference of the PMMA component for the oxide (plasma treated) silicon wafer substrate.[47] In previous studies of PS-*b*-PMMA thin films with a total relative molecular mass of 47.7 kg mol^{-1} and a mass fraction of PS of 0.74,[37,38] we mapped out two morphology transition lines separating the high and low temperature ordering regimes where the surface patterns suggest that the block copolymer cylinders are predominantly oriented parallel and perpendicular to the substrates, respectively, and forming an intermediate regime where these morphologies are strongly mixed. For example, in $h_f = 86$ nm BCP films, the parallel and perpendicular cylinders were observed at the temperatures above 155 °C and below 155 °C, respectively.[37] In other words, as we lower the temperature, the interfacial segregation strength increases leading to a transition between the two orientations. We now consider the same effect by varying the molecular mass in which our relatively low molecular mass BCPs have a parallel orientation. This should allow us to observe a parallel to perpendicular orientation transition if our interpretation of orientation dependence on interaction strength is correct.

Representative AFM height images of PS-*b*-PMMA block copolymers with different molecular masses are shown in Fig. 1. Evidently, the surface morphology of BCP thin films with different molecular masses can be controlled by adjusting the thermal history. In our previous works[37,38] a parallel cylinder BCP microphase orientation, which is natural given the wetting characteristics of the solid substrate for PMMA, is obtained by subjecting the BCP films to annealing at relatively high temperature (above 155 °C for the $h_f = 86$ nm thick BCP films). In Fig. 1a–c, we observe the formation of cylinders that are oriented perpendicular to the substrate by annealed the $M_n = 40.5$ kg mol^{-1}, 47.7 kg mol^{-1} and 77.5 kg mol^{-1} BCP films at 164 °C for 8 h. We then let an identical set of BCP films order by annealing them at relatively high temperature, 182 °C (Fig. 1d–f). We observe the formation of cylinders that are oriented parallel to the substrate in $M_n = 40.5$ kg mol^{-1} and 47.7 kg mol^{-1} BCP thin films after annealing at 182 °C for 8 h. For a 77.5 kg mol^{-1} BCP film, the surface pattern of perpendicular cylinder is observed at 182 °C. Clearly, for molecular masses in the relatively high molecular mass range, a perpendicular orientation cylindrical morphology is obtained. Furthermore, this perpendicular cylinder morphology remains stable and no significant morphological evolution is observed in our thin films on reasonable annealing timescales (several days). We previously studied the effect of the ordering temperature (T), film thickness (h_f) and film casting method on the surface morphology of cylinder-forming block PS-*b*-PMMA films,[37,38] the results of Fig. 1 are consistent with our previous paper if we take a horizontal T cut in the surface morphology phase diagram.

The cylinder-to-cylinder repeat distance (L_0) and corresponding layering distance of hexagonally packed cylinders (layer-to-layer, d) vary with the molecular mass of the BCP.[47] The layering distance of cylinders of the block copolymer is obtained by circularly averaging the two-dimensional power spectra of a Fast Fourier Transform (FFT) of the AFM image of a BCP surface pattern in a parallel cylinder orientation. The layering distance is evaluated from the relation, $d = 2\pi/q^*$, where q^* is the characteristic wave vector obtained from the peak in the FFT. For the asymmetric-wetting PS-*b*-PMMA BCP, *i.e.*, one block at the free surface and the other at the substrate interface, due to the commensurability constraint of film thickness with the layering distance, the film thickness is quantized to odd multiples of $d/2$, that is, $(2n + 1)d/2$, where n is an integer. If the initial film thickness is not commensurate with this constraint, an incomplete layer (islands or holes) of thickness d develops at

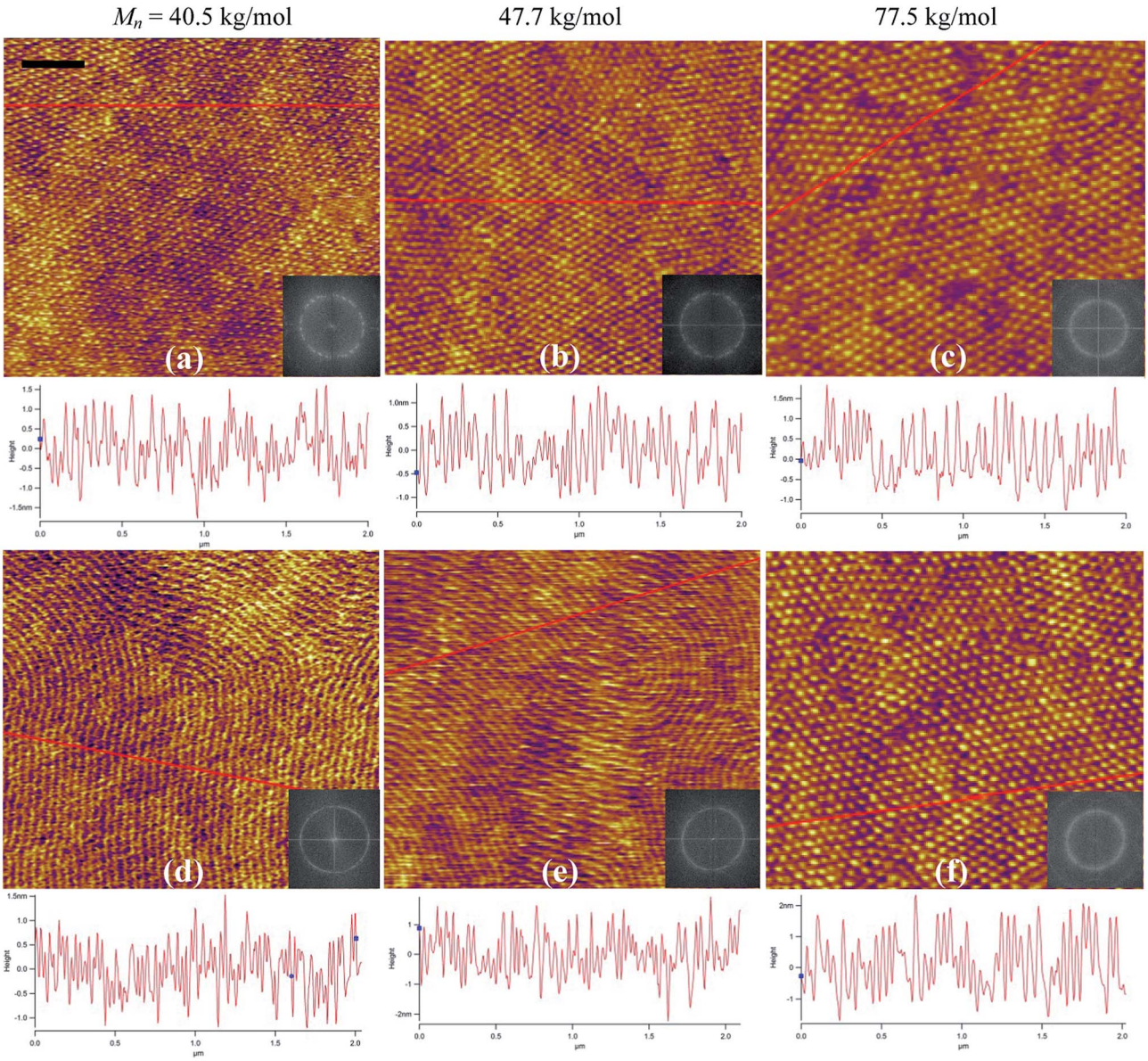

Fig. 1 AFM height images for PS-*b*-PMMA BCPs with M_n = 40.5 kg mol^{-1} (left column), and 47.7 kg mol^{-1} (center column) and 77.5 kg mol^{-1} (right column) after annealing for 8 h. Representative images of BCP film with h_f = 124 nm annealed at 164° C (a), h_f = 130 nm annealed at 164 °C (b), h_f = 141 nm annealed at 164 °C (c), h_f = 124 nm annealed at 182 °C (d), h_f = 130 nm annealed at 182 °C (e) and h_f = 141 nm annealed at 182 °C (f). The scale bar is 200 nm, and applies to all images. One dimensional height traces are provided below each AFM height image with corresponding position on the image indicated by a red line. Due to different cylinder repeat distances for PS-*b*-PMMA with different molecular masses, the film thickness slightly increases with M_n.

the free surface to maintain the natural period of cylinders.[48] The layering distance for M_n = 47.7 kg mol^{-1} PS-*b*-PMMA block copolymer is 23.4 nm and the corresponding repeat distance is ≈27 nm. For PS-*b*-PMMA sample with film thickness of 130 nm, which is commensurate with respect to the layering distance of the cylinders (≈5.5*d*), BCP cylinders in parallel and perpendicular orientations are observed at different annealing temperatures (shown in Fig. 1b and e). However, a 47.7 kg mol^{-1} PS-*b*-PMMA film having a thickness of 168 nm cannot accommodate an integral number of horizontally stacked cylinders (≈7.2*d*) in the parallel cylinder BCP microphase orientation and we show the impact of changing *T* on the ordered structure of these films in Fig. 2. As pointed out in our previous work,[48] only at the edge of incomplete layer the gradient change in thickness causes the close packing layers of cylinders to flip from the parallel to a perpendicular orientation in PS-*b*-PMMA film having cylinders oriented parallel to the substrate. This implies that the commensurability between the layering cylinder distance and the film thickness does not significantly influence cylinder orientation.

The scattering patterns obtained numerically by the two dimensional Fast Fourier Transform (2D FFT) of AFM images

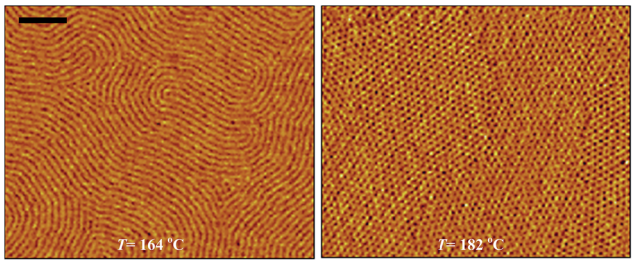

Fig. 2 AFM phase images for $M_n = 47.7$ kg mol^{-1} PS-*b*-PMMA with film thickness of 168 nm after annealing for 8 h. The scale bar is 200 nm, and applies to all images.

can be used to estimate the alignment of the BCP microstructures. If the aligned domains are randomly oriented, they would generate a uniform ring from the 2D FFT power spectra of AFM images. The isotropy of rings of FFT images shown as insets in Fig. 1 indicates the random distribution of aligned domains or the homogeneity of the alignment of the BCP microstructure. The aligned domain sizes for BCPs with $M_n = 40.5$ kg mol^{-1}, 47.7 kg mol^{-1} and 77.5 kg mol^{-1} after annealing at 164 °C for 8 h are 0.70 μm^2, 0.62 μm^2, 0.22 μm^2, respectively. The corresponding values for BCPs annealed at 182 °C for 8 h are 0.92 μm^2, 0.67 μm^2 and 0.27 μm^2. We see that a reduction in molecular mass leads to an increase in the aligned domain size, as expected.

The surface tension varies with molecular mass as, $\Upsilon = \Upsilon_\infty - k/M_n^{2/3}$, where Υ_∞ is the surface tension in the limit of infinite number-average molecular mass and k is a constant.[49] From this relation, it is evident that the surface tension increases monotonically with molecular mass. For a polymer having a molecular mass greater than (2 to 3) kg mol^{-1}, the surface tension reaches a plateau value.[49] For high mass polymers such as in our study (the molecular masses of PS and PMMA blocks are greater than 30.5 kg mol^{-1} and 10 kg mol^{-1}, respectively), the surface energy can be taken to be essentially constant. The near constancy should apply to the surface energy at both the polymer–air and polymer–substrate interfaces.

We obtained information about the internal ordering of nanostructures using neutron reflectometry. This technique involves measuring the intensity of reflected radiation as a function of wave vector, q. Neutron reflectometry provides detailed information about the average polymer composition profile normal to the plane substrate in thin film systems. Fig. 3 shows the representative NR curve for dPS-*b*-PMMA block copolymer film with a total relative molecular mass of 77.5 kg mol^{-1} and a mass fraction of dPS of 0.74. The cylinder repeat distance for this block copolymer is ≈38 nm and corresponding cylinder layering distance is 33 nm. The deuteration of the PS allows for a determination of the mass distribution of the two different polymer blocks as a function of film height (Z) (the air–polymer interface is at $Z = 0$). We used a fitting procedure to determine a completely free-form SLD profile within the film region. Detailed information about our fitting procedure is given in ref. 45. A careful alignment procedure is used for obtaining the most quantitative information on the internal ordering in BCP film, as can been seen from the sharp critical edge at low q in NR scan. The fit (red solid line) in this figure shows good agreement with data (black solid dots). The deep fringes up to high q indicate that the film is smooth (low roughness), which make the fit less uncertain. The overall film thickness, roughness and SLD can be extracted from the fit to the NR data. The solid line in the inset in the upper right of Fig. 3 is the best-fit SLD profile based on the NR data (high SLD corresponds to high dPS concentration). Nevertheless, a model

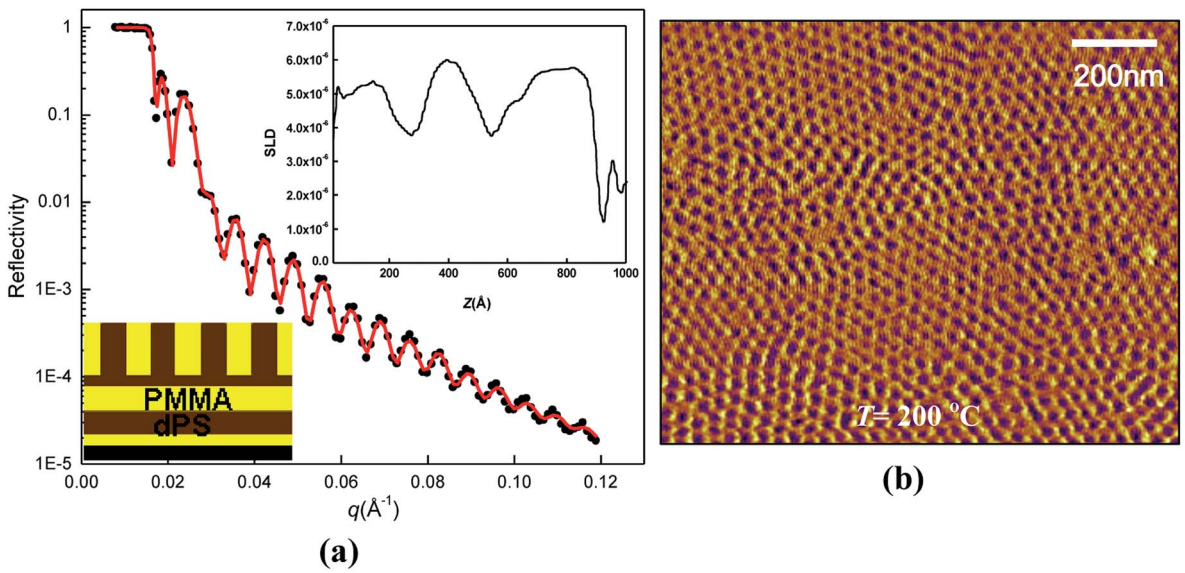

Fig. 3 Neutron reflectivity measurements on $M_n = 77.5$ kg mol^{-1} dPS-*b*-PMMA films with a perpendicular cylinder morphology at the surface (a) and corresponding AFM phase image is shown in (b). Neuron reflectivity scans (symbols) measured from a 96 nm BCP film after annealing for 15 h.

of a film with uniform SLD throughout its thickness (one-box model) is insufficient to reproduce the detailed NR decay implicit in the evident Kiessig fringes. A schematic BCP geometry is shown as an inset in the lower left of Fig. 3. From the SLD profile, the cylinder orientations within the BCP thin film can be obtained. NR data show a crossover between two different types of BCP morphologies (perpendicular and parallel cylinders). Near the solid substrate there is a wetting 'monolayer' with the thickness of 16 nm due to the preferential segregation of PMMA component of dPS-*b*-PMMA to the plasma-treated silicon wafer substrate. We further see that the perpendicular cylinder layer near the polymer–air interface extends about 20 nm into the film (flat region of the SLD curve). The center of the film between the wetting 'monolayer' and the perpendicular cylinder layer evidently exhibits a parallel-cylinder orientation. The oscillatory SLD curve reflects the periodic packing of cylinders parallel to the plane substrate. The thickness of the parallel cylinder layer is $\approx$60 nm. The corresponding AFM image shown in Fig. 3b indicates that the cylinders at the film surface are instead vertically oriented. The surface morphology of BCP film is consistent with neutron reflectivity.

A relatively new neutron scattering method, rotational small angle neutron scattering, is also used to obtain information about the internal ordering of nanostructure. In the method of rotational small angle neutron scattering, multiple transmission SANS measurements (the data is collected at each of the rotation angles.) are made on a single sample. The RSANS intensity is accumulated as a function of sample rotation angle. As the sample is rotated, the scattering pattern becomes sensitive to order along different planes through the scattering volume. Fig. 4 shows 2-dimensional slices of the 3-dimensional reconstructed reciprocal-space scattering intensity maps for the samples that exhibit the perpendicular cylinder morphology by AFM (see Fig. 1c). The toluene (casting solvent) is not deuterated in these measurements. The 2-dimensional intensity maps are plotted in a sample coordinate system, where the *z*-axis points in the film normal direction and the samples lies in the *x*–*y* plane. Thus the parallel cylinders extend in the *x*–*y* plane and have axes that point in *x*–*y* plane. The perpendicular cylinders are orthogonal. The axes of perpendicular cylinders point in the direction of the *z*-axis. The coordinates Q_x, Q_y, Q_z represent the position in reciprocal space. The corresponding fit to the data next to scattering intensity map allows a quantitative estimation of the relative contributions of parallel and perpendicular cylinder orientation populations. The 2-dimensional reconstructed reciprocal-space scattering intensity map shows a weak peak at $Q_x = 0.19\ \mathrm{nm}^{-1}$ (peak 1 in Fig. 4), which arises from the perpendicularly oriented cylinders within some angular distribution. The two intense vertical peaks at $Q_x = 0.16\ \mathrm{nm}^{-1}$ (peaks 2 in Fig. 4) are from the parallel, hexagonally packed cylinders. These three signals at $Q_x = 0.19\ \mathrm{nm}^{-1}$ and $0.16\ \mathrm{nm}^{-1}$ provide a measure of the perpendicular-oriented cylinder and the parallel-oriented cylinder populations, respectively. RSANS measures the entire film thickness and enables us to determine the BCP orientation within the film. The populations of cylinders oriented parallel to the substrate for BCP films annealed at 164 °C is 40% coverage. Due to a relatively strong affinity for PMMA to substrate and weak energetic preference for PS to segregate to the polymer–air interface, the air–polymer boundary becomes more susceptible. The selective interaction of PMMA for the solid substrate causes the BCP cylinders near this polymer–substrate boundary to orient parallel along the substrate. The uppermost layer can be reconstructed to form this new perpendicular cylinder morphology.

We also investigated the ordering of relatively high molecular mass BCPs. Fig. 5 shows AFM images of BCPs with M_n = 158.0 kg mol^{-1} and 367.2 kg mol^{-1}. In the range of annealing temperature (147 °C to 209 °C) and thickness (100 nm to 1200 nm) we investigated in this study, only perpendicular cylinder morphology is observed in high molecular mass BCPs (158.0 kg mol^{-1} and 367.2 kg mol^{-1}).

We next consider a three-dimensional view of the BCP film surface structure in Fig. 5 and 6. The relief can be appreciated from one-dimensional height traces obtained from AFM with the corresponding position on the image indicated by a red line in Fig. 1 and 5. The AFM height images indicate that the PMMA

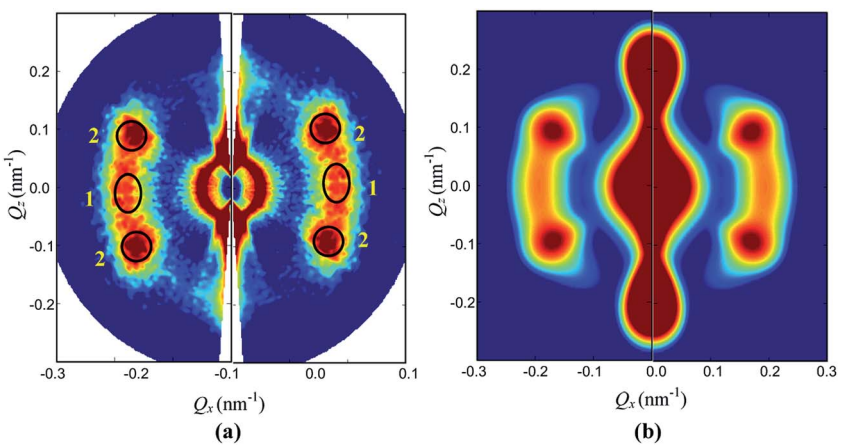

Fig. 4 Rotational small-angle neutron scattering (SANS) data (a) of dPS-*b*-PMMA block copolymers with film thickness of 141 nm annealed at 164 °C. The corresponding fits to the data (b) are provided.

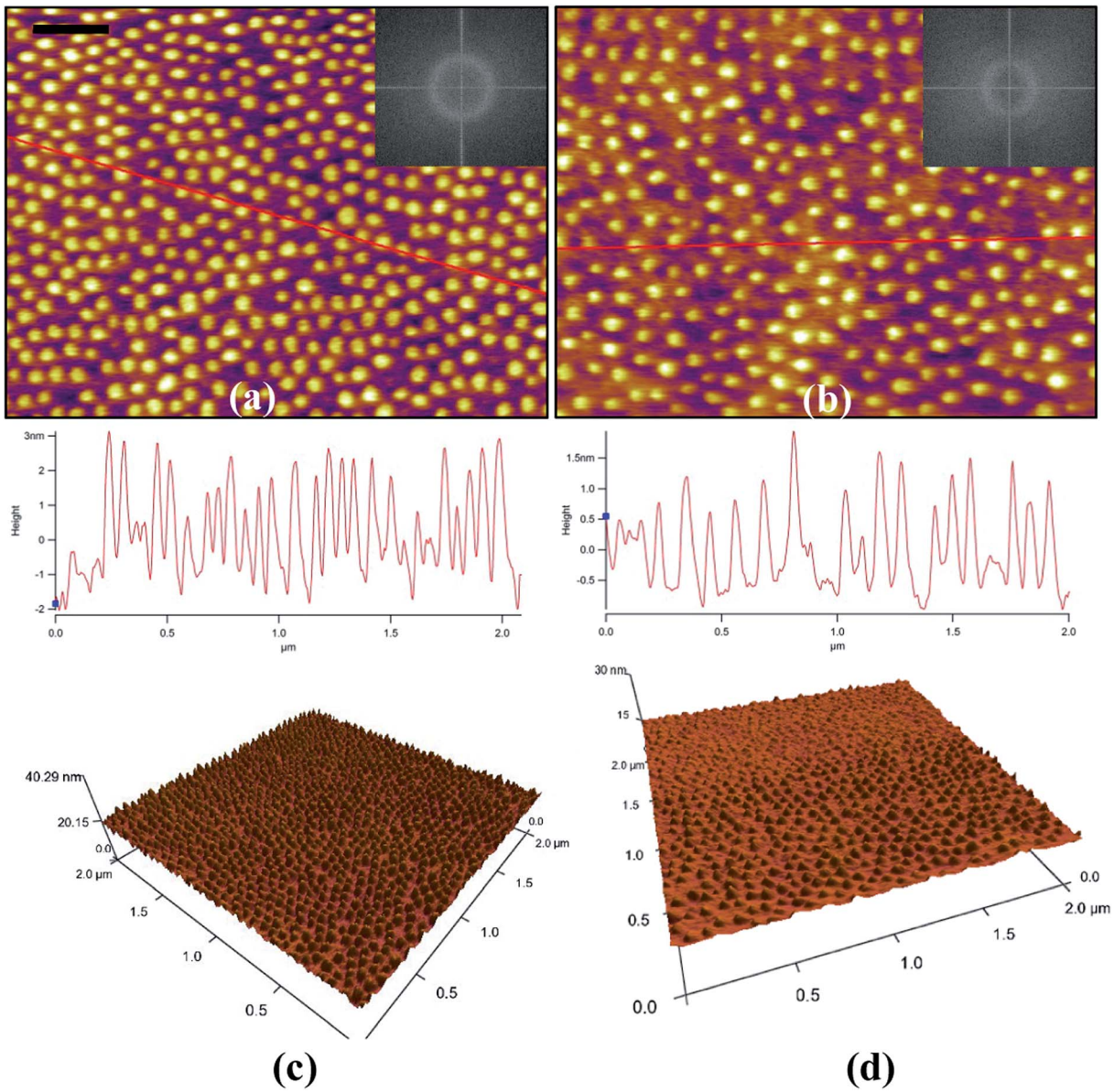

Fig. 5 AFM height images for PS-PMMA BCPs with $M_n = 158.0$ kg mol^{-1} (left) and 367.2 kg mol^{-1} (right) annealed at 182 °C for 15 h. Representative images of BCP films with $h_f = 167$ nm (a), $h_f = 165$ nm (b) and (c and d) 3D view of (a and b). The scale bar is 200 nm, and applies to panel (b). The 2D FFT of AFM image is indicated as inset.

cylinder regions are higher than the PS matrix. There is a small variation in the local film height with a peak to valley distance of 1 nm to 4 nm caused by the PMMA nanodomains. These height variations in the ordered BCP films are significant in comparison to as-cast BCP, where the root-mean-squared (RMS) roughness is relatively small (less than 0.6 nm). The amplitude of the polymer film thickness undulations increases with molecular mass of BCP (Fig. 7a).[50] The surface undulations in BCP film having a parallel cylinder microphase orientation at the free surface are somewhat more pronounced than in the BCP film with the perpendicular cylinders at the surface. These observations indicate that the polymer film thickness undulations are dependent on the surface orientation morphology.

To quantify the influence of molecular mass on the height variations of BCP films, the amplitude of the BCP film thickness undulations was normalized by the cylinder period distance. Fig. 7b shows this dimensionless ratio is an *invariant* in molecular mass in the wide range investigated (40.5 to 367.2) kg mol^{-1}. This phenomenon accords with our previous experience with phase separating polymer blends near their critical composition where the amplitude of the height fluctuations of the film divided by in-plane phase separation 'spinodal pattern' wavelength is an invariant in diverse blend systems.[51] We have observed this behavior in many blend pairs. In each case, the height undulation is a Marangoni-like effect[52] in that it has its origin in the surface tension differences between the polymer components and this origin can be demonstrated by adding a

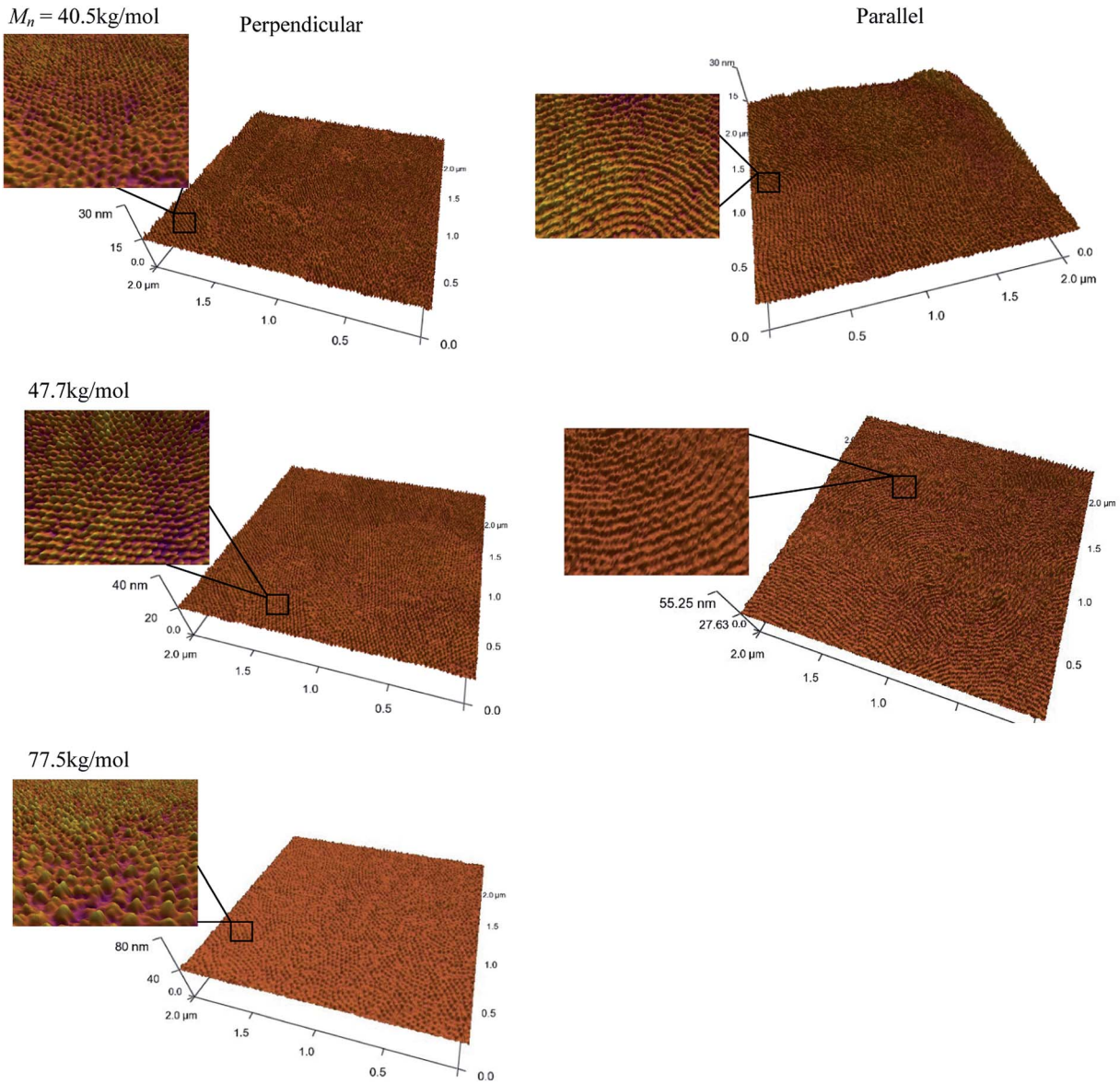

Fig. 6 Three dimensional view of AFM height images for PS–PMMA BCPs with M_n = 40.5 kg mol^{-1} (top row), 47.7 kg mol^{-1} (center row) and 77.5 kg mol^{-1} (bottom row). Perpendicular (left column) and parallel (right column) cylinders are shown. The perpendicular and parallel cylinder BCP orientations are obtained after annealing BCP films for 8 h at 164 °C and 182 °C, respectively. The thicknesses of 40.5 kg mol^{-1}, 47.7 kg mol^{-1} and 77.5 kg mol^{-1} BCP films are 124 nm, 130 nm and 141 nm, respectively.

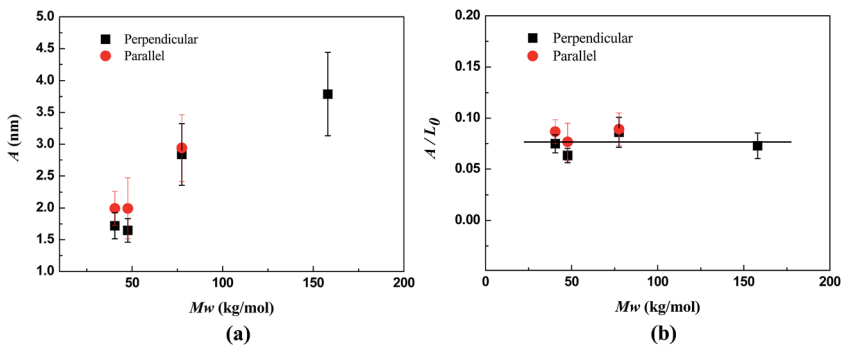

Fig. 7 (a) Amplitude (A) of film height undulations at the surface of BCP films having perpendicular and parallel cylinder orientations. (b) The normalized amplitude by the cylinder period distance.

little BCP to the blend, having the same homopolymers as the blend, which greatly reduces the interfacial energy difference and then completely levels the blend film.[53] We thus have a general method for engineering the well-controlled nanoscale fluctuations, both in height and in-plane pattern wavelength, through the control of the BCP molecular mass, which should be a useful tool in designing BCP films with targeted structure.

Next we consider the relationship between the in-plane pattern size and the BCP molecular mass. As pointed out previously,[47] the cylinder diameter, D, and corresponding cylinder repeat distance (cylinder-to-cylinder) vary with molecular mass. We measured the cylinder diameter and cylinder period distance of the block copolymer. The cylinder repeat distance is obtained by a FFT of the AFM image of a BCP surface pattern in a perpendicular cylinder orientation. The cylinder diameter and cylinder repeat distance increase with the molecular mass. Both scale with molecular mass of BCP with a power in the range 1/2 to 2/3 where the scale ratio D/L_0 is fairly constant, 0.50 ± 0.04 (Fig. 8). We can understand the enhancement of vertically oriented cylinders with increasing BCP mass very simply. Increasing the polymer mass increases the driving force for polymer ordering and BCP order–disorder transition temperature, but more importantly for the cylinder alignment problem, a larger χN also implies an increase of the *shear modulus* of the ordered BCP domains. By simply increasing BCP molecular mass at the same processing conditions we obtain robust perpendicular cylinder orientation. This effect is interpreted as arising from an enhancement of the BCP segregation strength as measured by χN and the associated change in the rigidity of the ordered BCP structures, which in turn implies an increase of the shear modulus of the ordered BCP domains. The segregation strength, χN, is important to this process since it controls the shear modulus of self-assembled BCP structures. The shear modulus is a significant factor in BCP alignment because this quantity controls the persistence length of the cylinders, as in the case of semi-flexible polymers. This relation between the stiffness of BCP materials and the magnitude of the block copolymer segregation strength, χN, is general in this class of materials and the measurement of the softening (as measured by the shear modulus) upon approaching the BCP order–disorder transition provides a convenient and often utilized rheological method for estimating BCP disordering temperature.[54,55] Cylinders formed from short BCP chains with small χN are thus understandably flaccid structures and tend to lay down parallel to the substrate, even if there is a weak selective polymer–substrate interaction rather than stand erect as the case when the cylinders are stiff, *i.e.*, large χN.

We have previously shown[37,38] that lowering temperature at a fixed film thickness can also lead to a greater alignment of cylinder domains normal to the film substrate, and recently, we have seen exactly the same effect with a PS–PMMA lamellae forming block copolymer material. In each case considered, we have evidence that increasing the molecular segregation strength, χN, and thus the stiffness of the assembled domains, stabilizes a BCP orientation perpendicular to the substrate, provided the interaction between the BCP and the substrate can be made nearly neutral. By combining the polymer–surface interaction and the rigidity of the BCP domains together, we can better control BCP morphology orientation. This offers a simple principle that can be used to engineer patterns with the desired morphology.

The addition of small molecule additives with a selective affinity for one of the blocks provides another strategy for increasing χN to enhance block copolymer ordering in thin films.[56,57] This approach to increasing segregation strength and the 'quality' of block copolymer ordering has recently been demonstrated in a number of bock copolymer materials[58–62] and Bennett *et al.*[63] have shown the applicability of this approach to ordering in the PS–PMMA block copolymer materials studied in the present paper where an ionic liquid that selectively complexes with the PMMA block was found to lead to large changes in χ.[59,60]

Of course, the practical use of high molecular mass polymers to enhance the perpendicular orientation of BCP materials is not without difficulties. We inevitably run up against complications associated with the slow rate of BCP ordering associated with film vitrification at low temperatures and the more serious problem of degradation of the quality of BCP ordering due to dynamic heterogeneity in glass-forming materials at low temperatures.[64] However, there are other ways of increasing block copolymer χN besides increasing molecular mass and decreasing temperature. The strategy of increasing χN through the introduction of low mass additives having a selective affinity for one of the blocks components then provides an attractive strategy for increasing χN and BCP morphology orientation when this approach is combined with a method of engineering the polymer–substrate interaction to be unselective. Bennett *et al.*[63] have already made progress in enhancing the ordering PS–PMMA block copolymer films using ionic liquid additives.

The robust vertical orientation of BCP films above a threshold molecular mass has important practical implications for many technological applications, including the development of highly selective and high-throughput (HS/HT) membranes by etching out the vertically ordered cylinders.

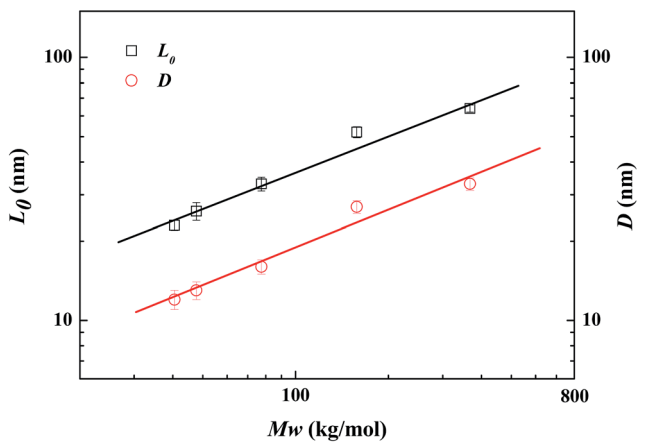

Fig. 8 Cylinder period distance (L_0) and cylinder diameter (D) as a function of molecular mass of BCP. Error bars were estimated from the standard deviation of repeated measurements.

Indeed future studies will report on their applications to oil–water separations studies.

Conclusions

We investigate the surface morphology of PS-*b*-PMMA thin films with different molecular mass that are of interest in nanomanufacturing applications. We find that we can robustly create BCP patterns with perpendicular cylinder orientation by simply increasing BCP molecular mass at the same processing conditions while the lower mass BCP cylinders orients parallel to the substrate. This effect is interpreted as arising from an enhancement of the BCP segregation strength, as measured by χN, and the associated change in the rigidity of the ordered BCP structures. Consistent with this interpretation of the flipping of cylinder orientation with molecular mass, we can now understand our previous observations showing a transition in cylinder orientation by reducing temperature as arising from the same effect.[37,38] In our most recent work, we have shown the same effect can also be achieved upon annealing at low temperatures ($\approx$140–165 °C) with lamellae-forming PS–PMMA BCP films when the polymer–surface interaction is rendered unselective through the use of nanoparticle additives. The strategy of controlling BCP orientation through the control of BCP segregation strength, χN, is apparently very general.

We also find that we can control the amplitude of the BCP film thickness undulations through tuning the BCP molecular mass and these changes scale linearly with the in-plane BCP pattern scale, which itself scales as a power of the BCP molecular mass. This relationship between in-plane pattern size and film roughness has been seen before in near-critical composition blend films, where the effect has been interpreted in terms of a balance of the ratio or surface to interfacial tension.[51] Our results together suggest that the perpendicular cylinder microphase orientation of high molecular mass BCP thin films at the free surface represents a thermodynamically stable state.

In previous work, we have also explored the effect of varying both temperature and block copolymer molecular mass on the in-plane interfacial pattern formation in thin block copolymer films of PS–PMMA forming lamellae oriented parallel to the substrate.[65–67] In these experiments, it was found that making the interfacial segregation strength, χN, stronger, either by lowering the temperature or by increasing the BCP molecular mass, had the effect of *reducing* the average scale of the interfacial pattern (holes, islands and 'spinodal' patterns depending on block copolymer film thickness), an effect attributed to an increased elastic energetic cost of deforming the block copolymer lamellae.[65–67] We conclude that this stiffening effect with increased mass and lowered temperature is key to the control of BCP lamellae and cylinder orientation in thin films as well.

Acknowledgements

The authors acknowledge financial support of National Basic Research Program of China (973 Program) (no. 2012CB821505), and National Natural Science Foundation of China (no. 21274103, and no. 21104054). We acknowledge the support of the National Institute of Standards and Technology, U.S. Department of Commerce, in providing the neutron research facilities used in this work. We also thank David Uhrig at Center for Nanophase Materials Sciences Division, Oak Ridge National Laboratory for help with the synthesis of the deuterated block copolymers and Ronald Jones at NIST and Kevin Yager at Brookhaven National Laboratory for help with RSANS measurements. AK would like to thank the ACS-PRF for funding in support of the work. AK also acknowledges support by the U.S. Department of Energy, Division of Basic Energy Sciences under contract no. DE-FG02-10ER4779 for the research.

References

1 M. J. Fasolka and A. M. Mayes, Block Copolymer Thin Films: Physics and Applications, *Annu. Rev. Mater. Res.*, 2001, **31**, 323–355.
2 C. J. Hawker and T. P. Russell, Block Copolymer Lithography: Merging "Bottom-Up" with "Top-Down" Processes, *MRS Bull.*, 2005, **30**, 952–966.
3 M. P. Stoykovich and P. F. Nealey, Block Copolymers and Conventional Lithography, *Mater. Today*, 2006, **9**, 20–29.
4 M. Li and C. K. Ober, Block Copolymer Patterns and Templates, *Mater. Today*, 2006, **9**, 30–39.
5 I. W. Hamley, Ordering in Thin Films of Block Copolymers: Fundamentals to Potential Applications, *Prog. Polym. Sci.*, 2009, **34**, 1161–1210.
6 S. B. Darling, Directing the Self-Assembly of Block Copolymers, *Prog. Polym. Sci.*, 2007, **32**, 1152–1204.
7 C. Harrison, M. Park, P. M. Chaikin, R. A. Register and D. H. Adamson, Lithography with a Mask of Block Copolymer Microstructures, *J. Vac. Sci. Technol., B: Microelectron. Nanometer Struct.–Process., Meas., Phenom.*, 1998, **16**, 544–552.
8 R. A. Segalman, Patterning with Block Copolymer Thin Films, *Mater. Sci. Eng., R*, 2005, **48**, 191–226.
9 H.-C. Kim, S.-M. Park and W. D. Hinsberg, Block Copolymer Based Nanostructures: Materials, Processes, and Applications to Electronics, *Chem. Rev.*, 2010, **110**, 146–177.
10 J. Y. Cheng, A. M. Mayes and C. A. Ross, Nanostructure Engineering by Templated Self-Assembly of Block Copolymers, *Nat. Mater.*, 2004, **3**, 823–828.
11 A. P. Marencic and R. A. Register, Controlling Order in Block Copolymer Thin Films for Nanopatterning Applications, in *Annual Review of Chemical and Biomolecular Engineering*, ed. J. M. Prausnitz, M. F. Doherty and M. A. Segalman, 2010, vol. 1, pp. 277–297.
12 B. Ashok, M. Muthukumar and T. P. Russell, Confined Thin Film Diblock Copolymer in the Presence of an Electric Field, *J. Chem. Phys.*, 2001, **115**, 1559–1564.
13 G. G. Pereira and D. R. M. Williams, Diblock Copolymer Melts in Electric Fields: The Transition from Parallel to Perpendicular Alignment Using a Capacitor Analogy, *Macromolecules*, 1999, **32**, 8115–8120.

14 Y. Tsori and D. Andelman, Thin Film Diblock Copolymers in Electric Field: Transition from Perpendicular to Parallel Lamellae, *Macromolecules*, 2002, **35**, 5161–5170.
15 P. Mansky, T. P. Russell, C. J. Hawker, M. Pitsikalis and J. Mays, Ordered Diblock Copolymer Films on Random Copolymer Brushes, *Macromolecules*, 1997, **30**, 6810–6813.
16 P. Mansky, T. P. Russell, C. J. Hawker, J. Mays, D. C. Cook and S. K. Satija, Interfacial Segregation in Disordered Block Copolymers: Effect of Tunable Surface Potentials, *Phys. Rev. Lett.*, 1997, **79**, 237–240.
17 E. Huang, L. Rockford, T. P. Russell and C. J. Hawker, Nanodomain Control in Copolymer Thin Films, *Nature*, 1998, **395**, 757–758.
18 E. Han, K. O. Stuen, M. Leolukman, C.-C. Liu, P. F. Nealey and P. Gopalan, Perpendicular Orientation of Domains in Cylinder-Forming Block Copolymer Thick Films by Controlled Interfacial Interactions, *Macromolecules*, 2009, **42**, 4896–4901.
19 B. L. Riise, G. H. Fredrickson, R. G. Larson and D. S. Pearson, Rheology and Shear-Induced Alignment of Lamellar Diblock and Triblock Copolymers, *Macromolecules*, 1995, **28**, 7653–7659.
20 K. A. Koppi, M. Tirrell and F. S. Bates, Shear-Induced Isotropic-to-Lamellar Transition, *Phys. Rev. Lett.*, 1993, **70**, 1449–1452.
21 S. H. Kim, M. J. Misner and T. P. Russell, Solvent-Induced Ordering in Thin Film Diblock Copolymer/Homopolymer Mixtures, *Adv. Mater.*, 2004, **16**, 2119–2123.
22 M. Kimura, M. J. Misner, T. Xu, S. H. Kim and T. P. Russell, Long-Range Ordering of Diblock Copolymers Induced by Droplet Pinning, *Langmuir*, 2003, **19**, 9910–9913.
23 R. A. Segalman, A. Hexemer and E. J. Kramer, Effects of Lateral Confinement on Order in Spherical Domain Block Copolymer Thin Films, *Macromolecules*, 2003, **36**, 6831–6839.
24 D. Sundrani, S. B. Darling and S. J. Sibener, Guiding Polymers to Perfection: Macroscopic Alignment of Nanoscale Domains, *Nano Lett.*, 2004, **4**, 273–276.
25 D. Sundrani, S. B. Darling and S. J. Sibener, Hierarchical Assembly and Compliance of Aligned Nanoscale Polymer Cylinders in Confinement, *Langmuir*, 2004, **20**, 5091–5099.
26 M. R. Hammond, E. Cochran, G. H. Fredrickson and E. J. Kramer, Temperature Dependence of Order, Disorder, and Defects in Laterally Confined Diblock Copolymer Cylinder Monolayers, *Macromolecules*, 2005, **38**, 6575–6585.
27 B. C. Berry, A. W. Bosse, J. F. Douglas, R. L. Jones and A. Karim, Orientational Order in Block Copolymer Films Zone Annealed Below the Order–Disorder Transition Temperature, *Nano Lett.*, 2007, **7**, 2789–2794.
28 K. G. Yager, N. J. Fredin, X. Zhang, B. C. Berry, A. Karim and R. L. Jones, Evolution of Block-Copolymer Order through a Moving Thermal Zone, *Soft Matter*, 2010, **6**, 92–99.
29 G. Singh, K. G. Yager, B. Berry, H.-C. Kim and A. Karim, Dynamic Thermal Field-Induced Gradient Soft-Shear for Highly Oriented Block Copolymer Thin Films, *ACS Nano*, 2012, **6**, 10335–10342.
30 G. Singh, K. G. Yager, D.-M. Smilgies, M. M. Kulkarni, D. G. Bucknall and A. Karim, Tuning Molecular Relaxation for Vertical Orientation in Cylindrical Block Copolymer Films *Via* Sharp Dynamic Zone Annealing, *Macromolecules*, 2012, **45**, 7107–7117.
31 J. Bodycomb, Y. Funaki, K. Kimishima and T. Hashimoto, Single-Grain Lamellar Microdomain from a Diblock Copolymer, *Macromolecules*, 1999, **32**, 2075–2077.
32 E. Sivaniah, Y. Hayashi, S. Matsubara, S. Kiyono, T. Hashimoto, K. Kukunaga, E. J. Kramer and T. Mates, Symmetric Diblock Copolymer Thin Films on Rough Substrates. Kinetics and Structure Formation in Pure Block Copolymer Thin Films, *Macromolecules*, 2005, **38**, 1837–1849.
33 Y. Tsori, E. Sivaniah, D. Andelman and T. Hashimoto, Orientational Transitions in Symmetric Diblock Copolymers on Rough Surfaces, *Macromolecules*, 2005, **38**, 7193–7196.
34 E. Sivaniah, Y. Hayashi, M. Iino, T. Hashimoto and K. Fukunaga, Observation of Perpendicular Orientation in Symmetric Diblock Copolymer Thin Films on Rough Substrates, *Macromolecules*, 2003, **36**, 5894–5896.
35 K. G. Yager, B. C. Berry, K. Page, D. Patton, A. Karim and E. J. Amis, Disordered Nanoparticle Interfaces for Directed Self-Assembly, *Soft Matter*, 2009, **5**, 622–628.
36 M. M. Kulkarni, K. G. Yager, A. Sharma and A. Karim, Combinatorial Block Copolymer Ordering on Tunable Rough Substrates, *Macromolecules*, 2012, **45**, 4303–4314.
37 X. Zhang, B. C. Berry, K. G. Yager, S. Kim, R. L. Jones, S. Satija, D. L. Pickel, J. F. Douglas and A. Karim, Surface Morphology Diagram for Cylinder-Forming Block Copolymer Thin Films, *ACS Nano*, 2008, **2**, 2331–2341.
38 X. Zhang, J. F. Douglas and R. L. Jones, Influence of Film Casting Method on Block Copolymer Ordering in Thin Films, *Soft Matter*, 2012, **8**, 4980–4987.
39 K. Y. Suh, Y. S. Kim and H. H. Lee, Parallel and Vertical Morphologies in Block Copolymers of Cylindrical Domain, *J. Chem. Phys.*, 1998, **108**, 1253–1256.
40 H. L. Khor, Y. Kuan, H. Kukula, K. Tamada, W. Knoll, M. Moeller and D. W. Hutmacher, Response of Cells on Surface-Induced Nanopatterns: Fibroblasts and Mesenchymal Progenitor Cells, *Biomacromolecules*, 2007, **8**, 1530–1540.
41 Certain equipment, instruments, or materials are identified in this paper in order to adequately specify the experimental details. Such identification does not imply recommendation by the NIST nor does it imply the materials are necessarily the best available for the purpose.
42 U. Jeong, D. Y. Ryu, D. H. Kho, J. K. Kim, J. T. Goldbach, D. H. Kim and T. P. Russell, Enhancement in the Orientation of the Microdomain in Block Copolymer Thin Films upon the Addition of Homopolymer, *Adv. Mater.*, 2004, **16**, 533–536.
43 D. Y. Ryu, S. Ham, E. Kim, U. Jeong, C. J. Hawker and T. P. Russell, Cylindrical Microdomain Orientation of PS-*b*-PMMA on the Balanced Interfacial Interactions: Composition Effect of Block Copolymers, *Macromolecules*, 2009, **42**, 4902–4906.

44 C. M. Stafford, K. E. Roskov, T. H. Epps and M. J. Fasolka, Generating Thickness Gradients of Thin Polymer Films *Via* Flow Coating, *Rev. Sci. Instrum.*, 2006, **77**, 023908.

45 C. F. Laub and T. L. Kuhl, Fitting a Free-Form Scattering Length Density Profile to Reflectivity Data Using Temperature-Proportional Quenching, *J. Chem. Phys.*, 2006, **125**, 244702.

46 W. Ruland and B. Smarsly, SAXS of Self-Assembled Nanocomposite Films with Oriented Two-Dimensional Cylinder Arrays: An Advanced Method of Evaluation, *J. Appl. Crystallogr.*, 2005, **38**, 78–86.

47 F. S. Bates and G. H. Fredrickson, Block Copolymer Thermodynamics – Theory and Experiment, *Annu. Rev. Phys. Chem.*, 1990, **41**, 525–557.

48 X. Zhang, K. G. Yager, J. F. Douglas and A. Karim, Suppression of target patterns in domain aligned cold-zone annealed block copolymer films with immobilized film-spanning nanoparticles, *Soft Matter*, 2014, **10**, 3656–3666.

49 S. Wu Surface and Interfacial Tensions of Polymers, Oligomers, Plasticizers, and Organic Pigments, in *Polymer Handbook*, ed. J. Brandrup, E. H. Immergut and E. A. Grulke, John Wiley and Sons, New York, 1999, pp. VI/521–VI/541.

50 The data in this manuscript, and in the figures, are presented along with the standard uncertainty involved in the measurement, where the uncertainty represents one standard deviation from the mean.

51 A. Karim, T. M. Slawecki, S. K. Kumar, J. F. Douglas, S. K. Satija, C. C. Han, T. P. Russell, T. P. Liu, R. Overney, J. Sokolov and M. H. Rafailovich, Phase-Separation-Induced Surface Patterns in Thin Polymer Blend Films, *Macromolecules*, 1998, **31**, 857–862; K. Dalnoki-Veress, J. A. Forrest and J. R. Dutcher, Mechanical confinement effects on the phase separation morphology of polymer blend thin films, *Phys. Rev. E: Stat. Phys., Plasmas, Fluids, Relat. Interdiscip. Top.*, 1998, **57**, 5811–5817.

52 L. E. Scriven and C. V. Sternling, The Marangoni Effects, *Nature*, 1960, **187**, 186–188.

53 L. Sung, A. I. Nakatani, C. C. Han, A. Karim, J. F. Douglas and S. K. Satija, The Role of the Copolymer Additives on Phase Behavior of a Polymer Blend, *Phys. B*, 1997, **241**, 1013–1015.

54 C. D. Han, D. M. Baek, J. K. Kim, T. Ogawa, N. Sakamoto and T. Hashimoto, Effect of Volume Fraction on the Order–Disorder Transition in Low Molecular Weight Polystyrene-*Block*-Polyisoprene Copolymers. (1) Order–Disorder Transition Temperature Determined by Rheological Measurements, *Macromolecules*, 1995, **28**, 5043–5062.

55 F. S. Bates, J. H. Rosedale and G. H. Fredrickson, Fluctuation effects in a symmetric diblock copolymer near the order–disorder transition, *J. Chem. Phys.*, 1990, **92**, 6255–6270.

56 J. Dudowicz, K. F. Freed and J. F. Douglas, Modification of the Phase-Stability of Polymer Blends by Diblock Copolymer Additives, *Macromolecules*, 1995, **28**, 2276–2287.

57 C. I. Huang and T. P. Lodge, Self-Consistent Calculations of Block Copolymer Solution Phase Behavior, *Macromolecules*, 1998, **31**, 3556–3565.

58 A. W. Bosse, V. R. Tirumala and E. K. Lin, Tuning Block Copolymer Phase Behavior with a Selectively Associating Homopolymer Additive, *J. Polym. Sci., Part B: Polym. Phys.*, 2009, **47**, 2083–2090.

59 J.-Y. Wang, W. Chen, C. Roy, J. D. Sievert and T. P. Russell, Influence of Ionic Complexes on Phase Behavior of Polystyrene-*B*-Poly(Methyl Methacrylate) Copolymers, *Macromolecules*, 2008, **41**, 963–969.

60 J.-Y. Wang, W. Chen and T. P. Russell, Ion-Complexation-Induced Changes in the Interaction Parameter and the Chain Conformation of PS-*B*-PMMA Copolymers, *Macromolecules*, 2008, **41**, 4904–4907.

61 V. R. Tirumala, A. Romang, S. Agarwal, E. K. Lin and J. J. Watkins, Well Ordered Polymer Melts from Blends of Disordered Triblock Copolymer Surfactants and Functional Homopolymers, *Adv. Mater.*, 2008, **20**, 1603–1608.

62 V. R. Tirumala, V. Daga, A. W. Bosse, A. Romang, J. Ilavsky, E. K. Lin and J. J. Watkins, Well-Ordered Polymer Melts with 5 nm Lamellar Domains from Blends of a Disordered Block Copolymer and a Selectively Associating Homopolymer of Low or High Molar Mass, *Macromolecules*, 2008, **41**, 7978–7985.

63 T. M. Bennett, K. Pei, H.-H. Cheng, K. J. Thurecht, K. S. Jack and I. Blakey, Can Ionic Liquid Additives Be Used to Extend the Scope of Poly(Styrene)-*Block*-Poly(Methyl Methacrylate) for Directed Self-Assembly?, *J. Micro/Nanolithogr., MEMS, MOEMS*, 2014, **13**, 031304.

64 A. W. Bosse, J. F. Douglas, B. C. Berry, R. L. Jones and A. Karim, Block-Copolymer Ordering with a Spatiotemporally Heterogeneous Mobility, *Phys. Rev. Lett.*, 2007, **99**, 216101.

65 A. P. Smith, J. F. Douglas, J. C. Meredith, E. J. Amis and A. Karim, Combinatorial Study of Surface Pattern Formation in Thin Block Copolymer Films, *Phys. Rev. Lett.*, 2001, **87**, 015503.

66 A. P. Smith, J. F. Douglas, J. C. Meredith, E. J. Amis and A. Karim, High-Throughput Characterization of Pattern Formation in Symmetric Diblock Copolymer Films, *J. Polym. Sci., Part B: Polym. Phys.*, 2001, **39**, 2141–2158.

67 A. P. Smith, J. F. Douglas, E. J. Amis and A. Karim, Effect of Temperature on the Morphology and Kinetics of Surface Pattern Formation in Thin Block Copolymer Films, *Langmuir*, 2007, **23**, 12380–12387.

